Bionatura Journal
Ibero-American Journal of Biotechnology and Life Sciences

Article

Functional Characterization of the STR3 Promoter under Exposure to the Pesticide Pyrimethanil: A Potential Tool for Environmental Monitoring

Paulo C. Robles-Ruiz [1, †], *Diana E. Arias-Arias* [1, †], *Francisco J. Álvarez* [1], *Alberto Aguirre-Bravo* [1], *Fernando A. Gonzales-Zubiate* [1, 2]

[1] *School of Biological Sciences and Engineering, Yachay Tech University, 100119, Urcuqui, Ecuador*
[2] *MIND Research Group, Model Intelligent Networks Development, Urcuqui, Ecuador*
**Correspondence author: fgonzales@yachaytech.edu.ec*
[†] *Both authors contributed equally to this work and are co-first authors*

ABSTRACT

The widespread use of fungicides in modern agriculture has intensified concerns about their ecological and toxicological impacts. At the same time, the lack of rapid, cost-effective detection methods continues to hinder routine monitoring of pesticide residues. Saccharomyces cerevisiae, with its well-characterized genetics and conserved stress-response pathways, offers a powerful platform for developing molecular biosensors. Previous transcriptomic studies have shown that exposure to the anilinopyrimidine fungicide pyrimethanil induces extensive transcriptional reprogramming in yeast, particularly affecting sulfur amino acid metabolism and associated stress-response networks. Among the most strongly upregulated genes is *STR3*, encoding cystathionine β-lyase, suggesting its potential as a sensitive reporter of fungicide-induced stress.

In this study, we constructed and validated a prom*STR3*::GFP reporter system to monitor *STR3* transcriptional activation in response to pyrimethanil exposure. Our results demonstrate a clear dose- and time-dependent increase in GFP fluorescence, accurately reflecting the physiological and metabolic disruption caused by the fungicide. This reproducible activation pattern highlights the *STR3* promoter as a promising molecular sensing element for the design of yeast-based biosensors.
Overall, our findings advance the understanding of cellular responses to pesticide stress in S. cerevisiae and substantiate the feasibility of leveraging promoter-reporter systems as low-cost, scalable tools for environmental and agricultural monitoring of fungicide contamination.
Keywords: pyrimethanil, gene expression, *Saccharomyces cerevisiae*, sustainable environment.

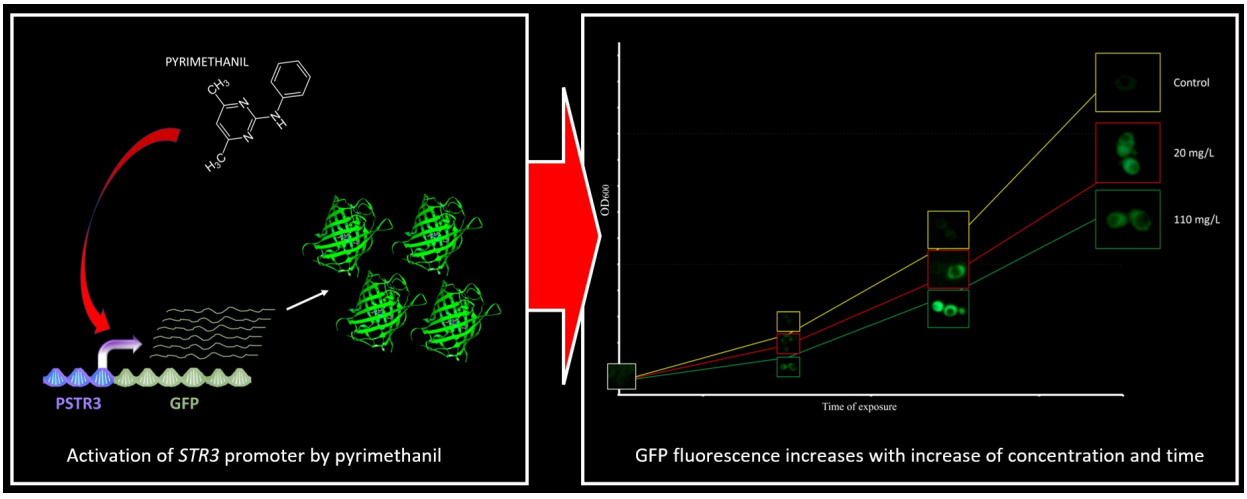

Graphical Abstract. A visual summary of the *STR3* promoter activation in response to pyrimethanil exposure

INTRODUCTION

Pesticides have played a crucial role in treating and preventing plant diseases, contributing significantly to increased crop yields and production. However, the dependence of our societies on these compounds represents one of the most critical challenges to environmental sustainability and public health [1,2]. One of the most widely used fungicides in agriculture is pyrimethanil (4,6-dimethyl-N-phenyl-2-pyrimidinamine) [3,4]. Pyrimethanil is a broad-spectrum anilinopyrimidine fungicide initially tested to manage gray mold (*Botrytis cinerea*) in vineyards and, over time, expanded to a variety of fruits and vegetables due to its exceptional efficacy and favorable safety profile [5,6]. Nevertheless, the persistence of pyrimethanil in the environment and its adverse effects on various ecosystems raise considerable concerns [7]. This fungicide has been linked to the toxic impacts on a range of organisms, including bacteria [8], yeast [9], arthropods [10], amphibians [11], fish [12], microalgae [13], and human cell lines [14]. These interactions underscore the necessity for a more comprehensive assessment of the risks associated with its use, aimed at mitigating its environmental impact and protecting the health of affected ecosystems.

S. cerevisiae appears as the most extensively utilized eukaryotic model within toxicological and ecotoxicological investigations, due to its intrinsic simplicity, deep evolutionary conservation, and the extensive repository of omics data available for this organism [15,16,17,18]. Its application has been essential for identifying biomarkers to evaluate the effects of environmental pollutants, including pesticides [19,20].

A significant example of pyrimethanil's impact on the *S. cerevisiae* transcriptomic profile was reported by Gil and collaborators, who identified genes responding to high concentrations of the fungicide [21]. Among these, the gene *STR3* was notably upregulated, underscoring its role in the yeast's response to pyrimethanil-induced stress. *STR3* (YGL184C) is an essential gene encoding cystathionine β-lyase, an enzyme that catalyzes the cleavage of cystathionine into homocysteine, ammonia, and pyruvate in a pyridoxal 5'-phosphate (PLP)-dependent manner [22,23,24]. This reaction is important because it serves as the forward transsulfuration pathway in the biosynthesis of methionine from cysteine (Figure 1).

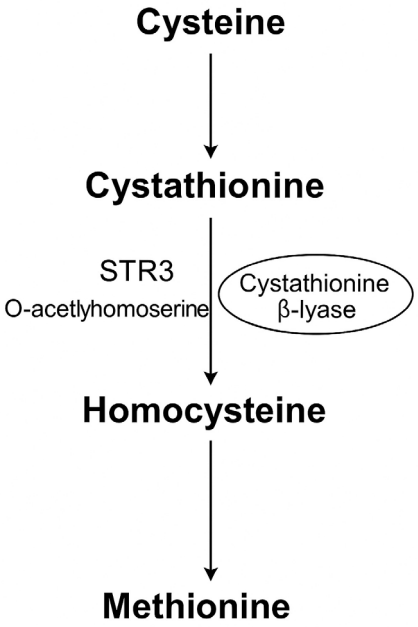

Figure 1. Schematic representation of the sulfur amino acid metabolic pathway showing the enzymatic steps leading from cysteine to methionine. Key intermediates, enzymes, and branch points relevant to *STR3* function are highlighted.

The regulation of *STR3* is influenced by the Met4p transcription factor, which is activated under conditions of sulfur limitation. Given that pyrimethanil can disrupt amino acid metabolism, potentially impacting sulfur assimilation pathways, it is plausible that the observed upregulation of *STR3* is a consequence of this metabolic stress. In *S. cerevisiae*, sulfur amino acid metabolism is tightly regulated and linked to overall sulfur metabolism. *STR3*, activated during sulfur starvation by the transcriptional activator Met4p and its cofactors [22], plays a key role in cellular sulfur balance and methionine biosynthesis.

In this work, we constructed a system using the inducible *STR3* promoter to drive GFP expression. The use of these specific promoters enables precise detection of pyrimethanil, providing an efficient approach for real-time monitoring. Furthermore, this system has the potential to expand beyond this pesticide to detect other environmental contaminants, offering a sustainable platform for broader agrochemical surveillance and ecological safety.

MATERIAL AND METHODS

Chemicals, strains, and growth media

The fungicide Lombardo® (pyrimethanil, 400 g/L) was obtained from Ningbo Sunjoy Agroscience Co., Ltd. (Ecuador) and applied at the concentrations indicated.

Genotypes of strains used in this study are described in Table 1. Bacterial maintenance and growth were performed in Luria-Bertani (LB) medium supplemented with ampicillin when necessary. Yeast maintenance and growth were performed in YPD medium (1% yeast extract, 2 % peptone, and 2 % glucose) or YNB medium (0.67 % yeast nitrogen base, 0.5 % $(NH_4)_2SO_4$, and 2 % glucose) supplemented with the required amino acids and nitrogenous bases [25].

Name	Characteristics/markers	Reference
DH5α	*E. coli; deoR endA1 gyrA96 hsdR17 Δ(lac)U169 recA1 relA1 supE44 thi-1*(φ80 *lacZΔ*M15)	ATCC
BY4742	*S. cerevisiae; MATα his3Δ1 leu2Δ0 lys2Δ0 ura3Δ0*	EUROSCARF
W303	*S. cerevisiae; MATa/MATα {leu2-3,112 trp1-1 can1-100 ura3-1 ade2-1 his3-11,15}*	EUROSCARF
BY/PSTR3	BY4742, 35-*promoterSTR3*	This study

Table 1. Strains used in this work

Genomic DNA extraction

Genomic DNA from S. cerevisiae W303 and BY4742 was isolated and purified as described by Sherman [25].

PCR Amplification

PCR Amplifications were performed in a 50 µl reaction volume consisting of 5 µl of 10X PCR Buffer (minus Mg), 1 µl of 10 mM dNTP mixture, 1.5 µl of 50 mM $MgCl_2$, 100 ng of *S. cerevisiae* genomic DNA, 1 µl of 10 µM of each primer, 1 Unit of Platinum Taq DNA Polymerase, and distilled water to 50 µl. Amplification of the *STR3* promoter was made with oligonucleotides 5'pSTR3inf and 3'pSTR3inf (Table 2). The thermocycler (Veriti, Applied Biosystems) was programmed for 1 min. of initial denaturation at 95 °C, followed by 25 cycles of 30 s at 95 °C for denaturation, and annealing 1 min. at 59 °C, extension for 30 s at 72 °C, and a final extension of 4 min. at 72 °C.

Name	Sequence	Reference
5'pSTR3inf	5'CAAAAGCTGGAGCTCGCCACACATCCCATAGCTCTGTGTG-3'	This study
3'pSTR3inf	5'CATGTCGAGGTCGACCTTTTTGCTTCTATGCTTTTGTTGTTTGC-3'	This study

Table 2. Oligonucleotides used in this work

Cloning

Plasmids used in this study were constructed using cloning techniques described by Green and Sambrook [26]. In silico strategies were made using Benchling (https://www.benchling.com/) and SnapGene

(https://www.snapgene.com/) platforms. Plasmid pUG35 [27] expressing *GFP* was modified by replacing the *MET25* promoter with *STR3* promoter.

Construction of plasmid 35-PSTR3 (Table 3): a 122 bp DNA fragment containing the *STR3* promoter was amplified by PCR and digested with the restriction enzymes SacI and SalI. Then, it was inserted by ligation into the vector pUG35, which had been previously digested with the same enzymes. Subsequent restriction analysis confirmed the successful cloning. The resulting plasmid expresses the *GFP* reporter under the regulation of the *STR3* promoter.

Plasmid name	Characteristics/markers	Reference
pUG34	*PMET25::yEGFP3, HIS3, CEN/ARS*	[27]
pUG35	*PMET25::yEGFP3, URA3, CEN/ARS*	[27]
35-PSTR3	pUG35, *promoterYGL184C::yEGFP*	This study

Table 3. Plasmids used in this work

DNA Purification and Analysis

Plasmid DNA was isolated and purified from DH5α cells using the GeneJet Plasmid Miniprep Kit (Thermo Scientific) according to the manufacturer's instructions (Thermo Scientific, 2024). DNA was analyzed by electrophoresis at 100 V for 30 min. in a 1% agarose gel prepared in 1x TAE buffer, and stained with ethidium bromide for visualization [26].

Preparation of electrocompetent bacterial cells

Electrocompetent E. coli DH5α cells were prepared following standard procedures [26]. Briefly, mid-log cultures (OD_{600} = 0.5–0.7) were harvested, washed repeatedly with ice-cold 10% glycerol, and concentrated to ~1–3 × 10^{10} cells/ml. Aliquots were stored at −80 °C until use.

Preparation of electrocompetent yeast cells

Electrocompetent BY4742 cells were generated according to Sherman [25] with minor modifications. Cultures grown to OD_{600} = 0.8–1.0 were washed with sterile water, treated with TE–lithium acetate and DTT, washed again, and finally resuspended in ice-cold 1 M sorbitol. Cells were kept on ice until electroporation.

Electroporation of *Escherichia coli*

Plasmid transformation of *E. coli* DH5α was performed via electroporation using a Gene Pulser Xcell (Bio-Rad) at 25 µF, 200 Ω, and 2.5–3.0 kV. After pulsing, cells were recovered in SOC medium at 37 °C for one h and plated on LB-ampicillin agar. Transformants were confirmed by restriction analysis [26].

Electroporation of *S. cerevisiae*

Electroporation of BY4742 was performed as described by Sherman [25]. Competent cells (40 µl) were mixed with 5–100 ng of plasmid DNA and pulsed in a 0.2 cm cuvette (25 µF, 200 Ω, 1.5 kV). Cells were immediately recovered in 1 M sorbitol at 30 °C for one hour and plated on selective YNB–sorbitol agar. Colonies appeared after 48–72 h.

Exposure to Pyrimethanil

All yeast strains were cultured in 25 ml of YNB glucose minimal medium supplemented with the required amino acids at 30 °C with constant orbital shaking at 160 rpm overnight. Subsequently, yeast cultures were adjusted to 0.2 OD_{600}, allowed to grow to 0.4 OD_{600}, and exposed to varying concentrations of pyrimethanil for different time periods. The pesticide was added as follows: 25 ml cultures were treated with corresponding volumes of 4, 8, 12, 16, and 88 µL of the fungicide at concentrations of 5, 10, 15, 20, and 110 mg/L, respectively. Samples were collected every 2 hours for microscopy and fluorescence analysis of *GFP* expression.

Sample Fixation for Fluorescence Microscopy

After exposure to pyrimethanil, 1 ml aliquots from each treatment were collected and centrifuged at 4000 x g for 5 min. The supernatant was discarded, and the cells were washed with sterile water and centrifuged again to ensure the complete removal of the culture medium. Cell pellets were resuspended in 10 µl of ice-cold methanol and 30 µl of ice-cold PBS, and incubated for 15 min at 4 °C. Then, samples were centrifuged at 435 x g for 1 min. The supernatant was discarded, and the pellet was washed with PBS. 5 µl of the cell suspension was placed on glass slides, and the edges of the coverslips were sealed with clear nail polish to prevent evaporation. The slides were stored at 4 °C, protected from light, for later observation under a fluorescence microscope (Leica DM4000B with LAS X software).

Fluorescence Intensity Analysis

For each of the 24 experimental conditions, two glass slides were prepared, and five visual fields were analyzed using a 40x objective lens. The images were captured in TIFF format with a resolution of 2560x1920 pixels. Fluorescence microscopy images were recorded with LAS X software (https://www.leica-microsystems.com). The most representative 10 cells per treatment were selected, and the analysis was performed with Fiji ImageJ software (https://imagej.net/software/fiji/). In the green channel, threshold adjustments, noise reduction, and processing tools were applied to highlight the cells of interest, with particles filtered within the size range of 5 to 12 µm. Quantitative values were obtained in triplicate for total intensity, average fluorescence, and integrated density from the defined regions of interest for each cell, as well as from background or noise intensity analysis. To obtain fluorescence intensity data, the "Measure" option was used within the regions of interest (ROIs), and the process was repeated three times per cell. This enabled the calculation of quantitative values, including total intensity, average fluorescence, integrated density, and the analyzed area. The same procedure was applied to the image background, in which the intensity of background noise or fluorescence was measured at three points. The background values were then subtracted from the fluorescence values measured in the cells to obtain more accurate readings. The Bright Field Transmitted Light (TL.BF) mode was used with an exposure time of 35.5 ms and a gain of 2.9; all other parameters were set to their default values. Subsequently, a specific *GFP* filter was employed with an exposure time of 600 ms and the same gain of 2.9.

RESULTS

Pyrimethanil induces extensive transcriptional remodeling in S. cerevisiae, and our results confirm and extend these observations. In our experimental system, the *STR3* promoter showed a clear, quantifiable response to pyrimethanil, validating its role as a sensitive reporter of fungicide-induced metabolic stress. This aligns with the transcriptomic analysis by Gil et al. [21], who reported differential expression of 777 genes following exposure to high pyrimethanil concentrations, including strong induction of genes involved in sulfur amino acid metabolism, arginine biosynthesis, oxidative stress defense, and multidrug resistance. *STR3* was among the most upregulated genes in their dataset, consistent with its involvement in sulfur pathway reconfiguration during chemical stress.

To characterize this response in real time, we constructed a GFP reporter driven by the *STR3* promoter and transformed it into *S. cerevisiae*, generating the BY/PSTR3 strain (Table 1). Cells were subsequently exposed to increasing concentrations of pyrimethanil, and promoter activity was monitored through fluorescence quantification. This system enabled a direct assessment of *STR3* activation dynamics, establishing a functional link between transcriptomic induction and real-time promoter responsiveness.

Pyrimethanil toxicity in *S. cerevisiae*

BY/PSTR3 culture was subjected to a range of pyrimethanil concentrations over a controlled time period to measure the fungicide effect on yeast growth. Figure 2 shows a growth curve for BY/PSTR3, in which growth was slightly reduced at concentrations ranging from low to moderate levels (5-15 mg/L), typically found in environmental residues. Still, yeast cells continued to proliferate, suggesting some degree of adaptation

(Figure 3). Higher concentrations of pyrimethanil (20 mg/L and 110 mg/L), mimicking potential agricultural misuse, caused severe growth impairment, indicating that the yeast cells were unable to recover from pyrimethanil's toxic effects.

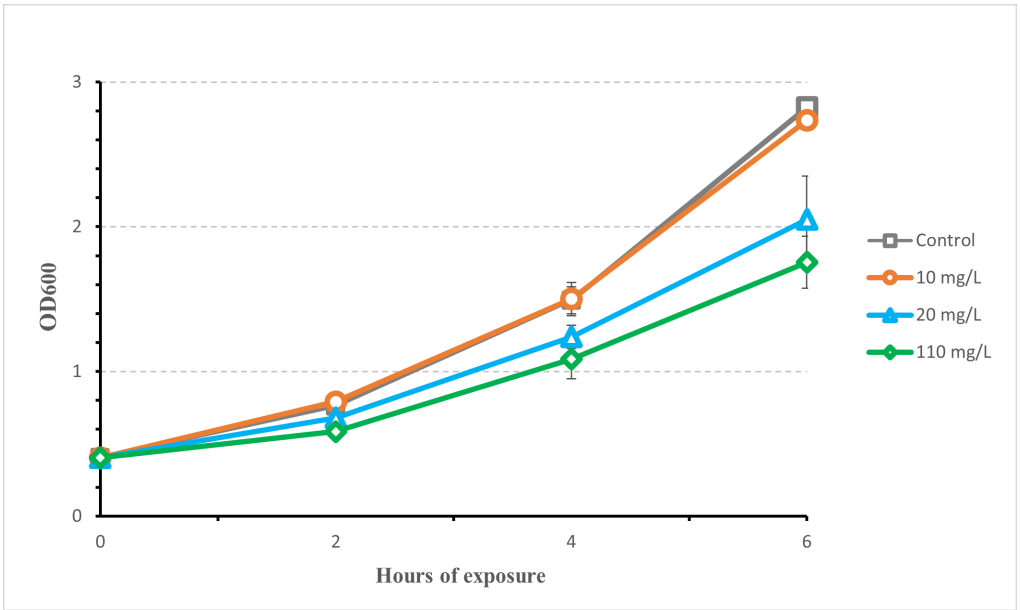

Figure 2. Growth kinetics of *S. cerevisiae* BY/PSTR3 exposed to increasing pyrimethanil concentrations. Optical density (OD_{600}) measurements were collected over time to assess the impact of pyrimethanil on yeast proliferation. The figure displays growth curves for each concentration, illustrating dose-dependent inhibition and temporal progression.

GFP expression driven by the *STR3* promoter was augmented

The activity of *the STR3* promoter was assessed by measuring GFP fluorescence in *S. cerevisiae* cells. *GFP* expression in the BY/PSTR3 strain increased progressively with higher concentrations of pyrimethanil.

The prom*STR3*::GFP reporter system demonstrated strong and selective activation in response to pyrimethanil, producing distinct fluorescence patterns that depended on both exposure duration and fungicide concentration. Statistical validation using Type III two-way ANOVA confirmed highly significant effects of exposure time ($F(3,384) = 6.53$, $p = 0.000256$) and pyrimethanil concentration ($F(5,38) = 3.49$, $p = 0.004251$), as well as a particularly robust interaction between these factors ($F(15,384) = 8.18$, $p = 3.56 \times 10^{-13}$). These results demonstrate that *STR3*-driven GFP expression exhibits a dynamic induction pattern shaped by both dose and exposure time.

Post hoc comparisons further clarified the specific differences among treatments, and the promoter's temporal behavior at each concentration is summarized in Table 4.

Conc. (mg/L)	Time				Experimental Confirmation
	0 h	2 h (vs Ref)	4h (vs Ref)	8 h (vs Ref)	
0	Reference	+24.41***	+18.85**	11,06	No observable fluorescence
5	Not significant	+41.67***	+36.67**	22,99	Mild early activation
10	Not significant	+55.60***	+52.69***	+24.93**	Notable increase from 2 h
15	Not significant	+50.43***	+68.38***	+52.48***	Sustained progressive response
20	+15.31*	+53.35***	+67.92***	+34.84***	Faint fluorescence at 0 h, then pronounced
100	+22.56*	+83.17***	+103.67***	+20.52*	Faint fluorescence at 0 h, then intense

Table 4. Time-dependent fluorescence induction of the *STR3* promoter in BY/PSTR3 cells exposed to varying pyrimethanil concentrations (*p < 0.001, **p < 0.01, *p < 0.05 vs 0 hours).**

As shown in Figures 3 and 4, the quantitative fluorescence data at 0 hours corroborated the microscopic observations, exhibiting only a faint signal at 20 mg/L (+15.31 units, $p = 0.072$) and 110 mg/L (+22.56 units, $p = 0.011$), while bright-field images confirmed normal cell morphology under all conditions. This low baseline is consistent with minimal *STR3* promoter activation or residual GFP signal.

By 2 hours of exposure—coinciding with the first microscopically detectable fluorescence—concentrations ≥10 mg/L showed significant induction, with responses ranging from 50.43 ± 7.03 units (15 mg/L, $p < 0.001$) to 83.17 ± 10.42 units (110 mg/L, $p < 0.001$). This interval corresponds to the initial activation phase of the *STR3* promoter, during which cells exposed to 10–15 mg/L exhibited a clear increase in signal intensity.

The optimal reading point was identified at 4 hours, when both maximal fluorescence and the greatest discriminatory capacity between concentrations were observed. At this time, 110 mg/L produced 103.67 ± 8.35 units ($p < 0.001$), significantly higher than all other treatments, including 20 mg/L (difference: 43.00 ± 8.80 units, $p < 0.001$). This window also corresponds to a stage in which cells at 110 mg/L exhibited stronger fluorescence and subtle morphological changes, indicative of active—but not yet critical—stress responses.

Interestingly, the response at 110 mg/L exhibited a biphasic profile: a strong induction at 4 hours (103.67 ± 8.35 units, $p < 0.001$), followed by a marked decrease at 8 hours (an 83.15 ± 7.48-unit decrease from T_4, $p < 0.001$). This regression coincided with the most pronounced morphological alterations observed microscopically, suggesting either saturation of the stress-response pathway or the onset of cellular toxicity.

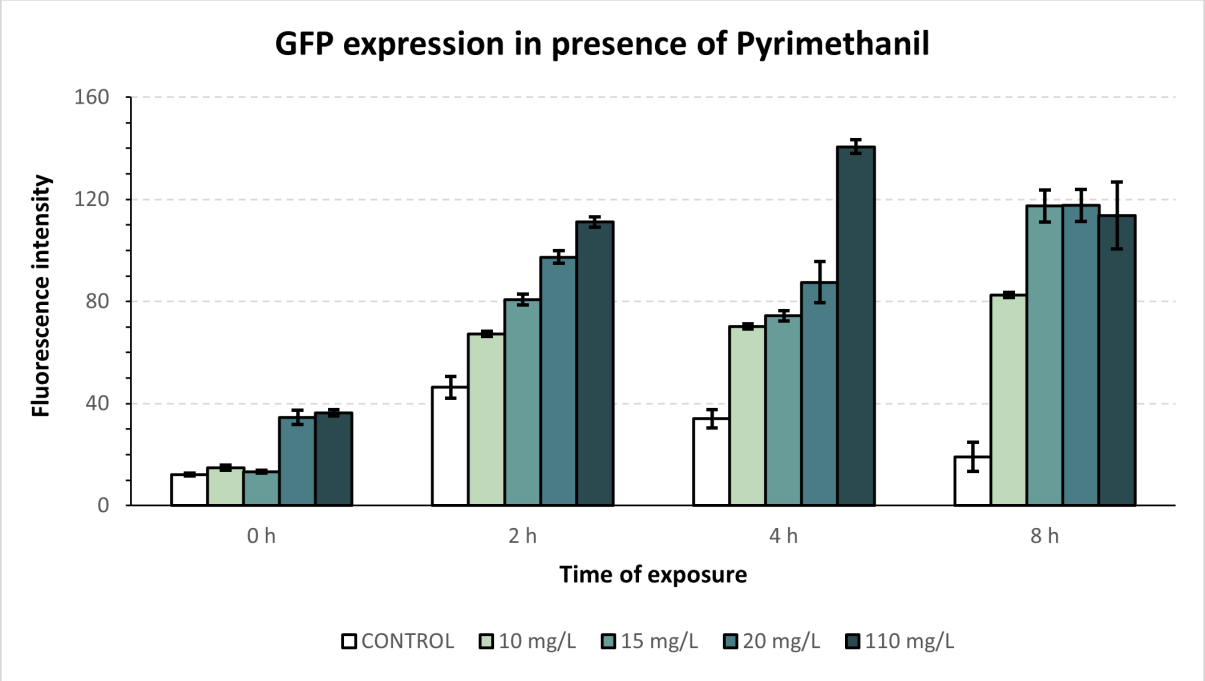

Figure 3. Time- and dose-dependent GFP fluorescence in *S. cerevisiae* BY/PSTR3 exposed to pyrimethanil.
This panel shows quantitative fluorescence measurements of STR3-driven GFP expression across multiple pyrimethanil concentrations and exposure times. Error bars represent SEM (n = 3 biological replicates). The figure illustrates promoter activation dynamics across conditions.

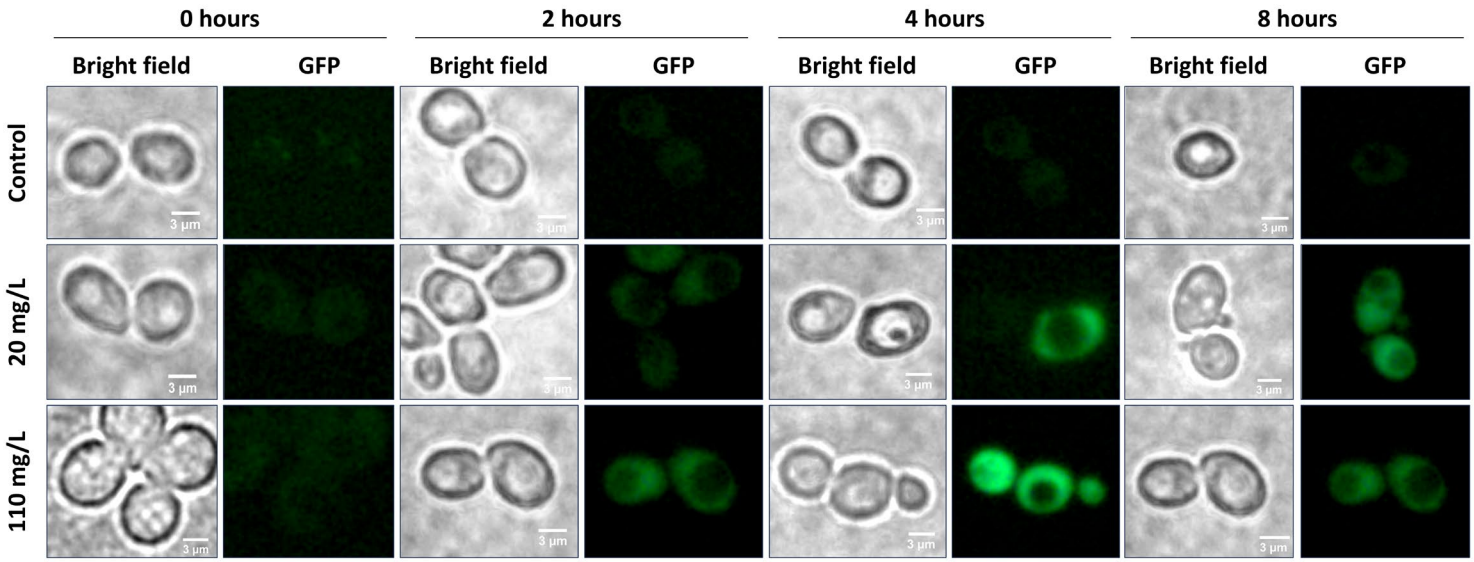

Figure 4. Fluorescence and bright-field microscopy images of *S. cerevisiae* BY/PSTR3 showing *STR3* promoter activation under pyrimethanil exposure. Representative microscopy images captured at various time points and pyrimethanil concentrations. Fluorescence panels display GFP expression driven by the *STR3* promoter, while corresponding bright-field images show cell morphology. Images were acquired under identical exposure settings.

Overall, *STR3*-driven GFP expression increased in a clear time- and dose-dependent manner upon pyrimethanil exposure. The strongest induction occurred at 110 mg/L, underscoring the *STR3* promoter's sensitivity to fungicide-induced stress. These findings reinforce the potential of *STR3* as a robust sensing element for future pesticide-responsive biosensors (Table 5).

Evaluation Parameter	2 hours	4 hours	8 hours	Interpretation and Recommendation
Limit of Detection	10 mg/L	5 mg/L	15 mg/L	Maximum sensitivity at 4 hours
Maximum Signal (vs control)	+81.3 units (110 mg/L)	+107.4 units (110 mg/L)	+39.1 units (20 mg/L)	Maximum fluorescence at 4 hours
Response Stability	Active induction phase	Expression peak	Decay at high concentrations	Optimal window: 2-4 hours

Table 5. Sensitivity parameters of the prom*STR3*::GFP reporter system for pyrimethanil detection as a function of exposure time.

DISCUSSION

The findings presented in this study provide compelling evidence that the *STR3* promoter in *S. cerevisiae* functions as a reliable and sensitive biosensor for detecting pyrimethanil-induced stress. The dose-dependent upregulation of GFP expression in the BY/PSTR3 strain highlights both the promoter's specificity and responsiveness to the fungicide's toxic effects. At a concentration of 20 mg/L, pyrimethanil begins to exert measurable metabolic stress, triggering activation of sulfur-related stress-response pathways; this is reflected in the progressive increase in the GFP signal, which peaks at 110 mg/L. These observations are consistent with previous transcriptomic analyses showing that pyrimethanil strongly perturbs sulfur amino acid metabolism and induces *STR3* among the most upregulated genes in *S. cerevisiae* [20,28].

The mechanism of action of pyrimethanil—linked to disruption of sulfur amino acid metabolism and inhibition of key enzymes—leads to metabolic imbalance in yeast cells. This disturbance activates downstream genes in the transsulfuration and sulfur assimilation pathways, including *STR3*, whose promoter elicits a clear, quantifiable fluorescence signal. Our results demonstrate a strong correlation between pyrimethanil

concentration and *STR3*-driven GFP expression, supporting the use of this promoter as a core sensing module in whole-cell biosensors. This is in line with recent systems-level studies showing that sulfur metabolism genes are central nodes in yeast responses to chemical and multi-stress conditions [28,29].

The choice of promoter is a critical design parameter in yeast-based biosensors, as it determines the balance between sensitivity, specificity, and background noise [30,31]. In this context, our results allow a functional comparison of *STR3* with other promoters frequently used in *S. cerevisiae* biosensors. The *MET25* promoter is strongly induced under methionine limitation and has been exploited not only as a regulatable expression system but also for metal and lead sensing; however, its activity is heavily influenced by global sulfur status, which can complicate interpretation in complex environmental samples [32]. The *CUP1* promoter is among the most widely used metal-responsive promoters. It underpins several copper biosensors that employ colorimetric, fluorometric, and electrochemical readouts, including recent next-generation designs with improved signal-to-noise and portable formats [33-36]. In contrast, *HSP12* is a prototypical general stress promoter activated by heat, osmotic stress, ethanol, oxidative stress, and the stationary phase. It has been used to monitor global stress status rather than specific toxicants [37-39].

While *MET25*, *CUP1*, and *HSP12* are powerful tools, their induction profiles are strongly influenced by multiple stressors.
In comparison, the *STR3* promoter offers several advantages: (i) it is mechanistically linked to the specific perturbation of sulfur amino acid metabolism caused by pyrimethanil, rather than to general nutritional or metal stress; (ii) it displays a clear dose- and time-dependent induction pattern with relatively low basal noise; and (iii) its regulation is consistent with transcriptomic signatures specifically associated with anilinopyrimidine fungicide exposure [20,40].

These features are desirable in modern transcription factor- and promoter-based biosensors, where minimizing cross-responsiveness and background activation is essential for quantitative interpretation [41,42].
The relevance of yeast-based biosensing platforms for environmental monitoring is further reinforced by recent work from Mendes et al., who engineered *S. cerevisiae* strains carrying fungicide-responsive promoters to detect tebuconazole with high specificity and low detection limits, and later highlighted the broader potential of biosensors in pesticide monitoring within aquatic environments [20,43]. In parallel, several reviews and case studies have emphasized the advantages of yeast-based whole-cell biosensors—such as low cost, scalability, and compatibility with optical or electrochemical detection—for environmental and toxicological applications [30,36,44,45].

Our *STR3*-based system fits within this evolving landscape by providing a mechanistically informed, promoter-driven biosensor tailored to anilinopyrimidine fungicides.
Future work should refine the analytical performance of the *STR3* promoter-based biosensor, including the formal determination of the limit of detection (LOD), limit of quantification (LOQ), precision (coefficient of variation), and accuracy (recovery assays) in buffer and real matrices such as water and soil extracts. Given the growing interest in promoter engineering and signal amplification circuits to enhance yeast biosensor sensitivity and dynamic range [41,46], *STR3* could also be integrated into synthetic promoter architectures or cascaded circuits to improve responsiveness at lower pyrimethanil concentrations. Additionally, testing *STR3* activation in the presence of structurally related anilinopyrimidine fungicides (e.g., cyprodinil, mepanipyrim) will be essential to define its specificity window and potential use in multiplexed detection systems.

In practice, the STR3-based reporter system shows strong potential as a rapid, sensitive, and cost-effective tool for monitoring pyrimethanil contamination in agricultural and environmental settings. Combined with emerging advances in yeast immobilization, portable readout platforms, and microplate-based high-throughput assays [47,48], this promoter–reporter module could contribute to next-generation biosensor technologies for pesticide surveillance and environmental risk assessment.

CONCLUSIONS

This study demonstrates that the *STR3* promoter fused to a GFP reporter is a functional and sensitive system for detecting pyrimethanil-induced stress in S. cerevisiae. The dose-dependent fluorescence response reliably reflected the fungicide's effects, confirming that *STR3* activation can serve as an effective proxy for cellular stress induced by pyrimethanil exposure. The consistently elevated fluorescence above basal levels highlight the potential of this promoter–reporter system as a scalable biosensing platform for environmental monitoring. Future work should refine the biosensor's analytical performance, including the determination of precise detection and quantification limits, and evaluate it across diverse environmental matrices and ecological conditions. Yeast-based biosensors, such as this one, offer promising advantages for the rapid, accurate, and cost-effective detection of environmental contaminants. Overall, the results presented here establish a solid foundation for the development of next-generation biosensor technologies and position the *STR3* promoter as a strong candidate for applications in environmental surveillance and pesticide monitoring.

Funding Statement
This research received internal funding from Yachay Tech University, Grant PII24-03, awarded to F.A.G.Z. and F.J.A. D.E.A.A. was supported by the SENESCYT Master's Fellowship ARSEQ-BEC-004596-2022.
No external funding was received.

Conflict of Interest Statement
The authors declare no conflict of interest.The funding institutions had no role in the study design; data collection, analysis, or interpretation; manuscript writing; or the decision to submit the work for publication.

Author Contributions: For research articles with multiple authors, a short paragraph outlining each author's individual contributions must be provided. The following statements should be used Conceptualization, F.A.G.Z. and F.J.A.; methodology, F.A.G.Z. and F.J.A.; validation, D.E.A.A. and P.C.R.R.; formal analysis, D.E.A.A. and P.C.R.R.; investigation, D.E.A.A., P.C.R.R., F.A.G.Z. and F.J.A.; resources, F.A.G.Z. and F.J.A.; data curation, D.E.A.A. and P.C.R.R.; writing—original draft preparation, D.E.A.A. and P.C.R.R.; writing—review and editing, D.E.A.A., P.C.R.R., A.A.B., F.A.G.Z. and F.J.A.; supervision, F.A.G.Z. and F.J.A..; project administration, F.A.G.Z.; funding acquisition, F.A.G.Z. and F.J.A.

Funding: This research was funded by Yachay Tech University Grant PII24-03 (to F.A.G.Z. and F.J.A.), D.E.A.A. was the recipient of SENECYT Master's Fellowship ARSEQ-BEC-004596-2022.

Acknowledgments: We would like to express our sincere gratitude to Yachay University for the financial support given to the project PII24-03 through the Internal Call for Research Project Funding 2024. To the laboratory of the School of Biological Sciences and Engineering for providing the facilities and resources necessary for the completion of this work. We are especially grateful to technicians Belen, Denis, Isaac, and Genesis for their invaluable technical assistance and constant support throughout the experiments.

Conflicts of Interest: The authors declare no conflicts of interest.

Data Availability Statement

The datasets generated and analyzed during this study are available from the corresponding author upon reasonable request.

Institutional Review Board Statement

Not applicable. This study did not involve humans or animals.

Informed Consent Statement

Not applicable. No human subjects were involved in this research.

Acknowledgments

The authors thank Yachay Tech University for supporting Project PII24-03 through the Internal Call for Research Project Funding 2024, and the School of Biological Sciences and Engineering for providing laboratory

facilities and essential technical resources.
We also acknowledge the invaluable assistance of technicians Belén, Denis, Isaac, and Genesis, whose support greatly facilitated experimental execution and data acquisition.

Biosafety Considerations

All work involving recombinant *Saccharomyces cerevisiae* was conducted under BSL-1 containment, in accordance with standard biosafety procedures.
All cultures and materials that came into contact with recombinant strains were autoclaved at 121 °C for 20 minutes before disposal.
Waste containing pyrimethanil or other fungicides was handled separately, properly labeled, and disposed of through certified hazardous-waste management systems to prevent environmental contamination.

AI-Assisted Tools Disclosure

No artificial intelligence system was used to generate, manipulate, or analyze experimental data, images, fluorescence measurements, or statistical output in this study. All experimental procedures, microscopy analyses, and quantitative assessments were performed directly by the authors using validated scientific methods.

Generative AI tools were used exclusively for minor linguistic refinement and formatting standardization of the manuscript, under full human supervision.
No AI tool contributed to scientific interpretation, data generation, experimental design, or the creation of original scientific content.
The authors independently verified all results, analyses, and conclusions in accordance with BioNatura Journal's policy on AI-assisted content:https://bionaturajournal.com/artificial-intelligence--ai-.html

Biosafety Considerations

All work involving recombinant Saccharomyces cerevisiae was conducted under BSL-1 conditions, in accordance with standard safety practices for non-pathogenic yeast. Cultures and materials that came into contact with recombinant strains were autoclaved (121 °C, 20 min) before disposal. Waste containing pyrimethanil or other fungicides was collected separately, labeled, and disposed of in accordance with certified hazardous-waste procedures to prevent environmental contamination.

Applicability to Environmental Matrices and Specificity

Although validated under laboratory conditions, this prototype may be applied to real samples such as water or soil extracts, pending assessment of potential matrix effects. Because pyrimethanil belongs to the anilinopyrimidine class of fungicides, specificity tests against related compounds will be necessary to confirm selectivity and avoid cross-reactivity in complex environmental settings.

REFERENCES

1. Mollocana Lara EC, Gonzales-Zubiate FA. Control of pesticides in Ecuador: An underrated problem? Bionatura. 2020;5(3):1257–63. doi:10.21931/RB/2020.05.03.17

2. Tsalidis GA. Human health and ecosystem quality benefit from life cycle assessment due to the elimination of fungicides in agriculture. Sustainability. 2022;14(2):846. doi:10.3390/su14020846

3. Rosslenbroich HJ, Stuebler D. Botrytis cinerea—history of chemical control and novel fungicides for its management. Crop Prot. 2000;19(8):557–61. doi:10.1016/S0261-2194(00)00072-7

4. Shao W, Zhao Y, Ma Z. Advances in understanding fungicide resistance in Botrytis cinerea in China. Phytopathology. 2021;111(3):455–63. doi:10.1094/PHYTO-07-20-0313-IA

5. Eberlin AR, Frampton CS. A metastable polymorphic form of the antifungal anilinopyrimidine pyrimethanil. Acta Crystallogr E Crystallogr Commun. 2017;73:886–9. doi:10.1107/S2056989017007563

6. Cabras P, Angioni A, Garau VL, Melis M, Pirisi FM, Minelli EV, et al. Fate of new fungicides (cyprodinil, fludioxonil, pyrimethanil, and tebuconazole) from vine to wine. J Agric Food Chem. 1997;45(7):2708–10. doi:10.1021/jf960939x

7. Chen Z, Dong X, Liu C, Wang S, Dong S, Huang Q. Rapid detection of residual chlorpyrifos and pyrimethanil on fruit surfaces using surface-enhanced Raman spectroscopy integrated with deep learning. Sci Rep. 2023;13:45954. doi:10.1038/s41598-023-45954-y

8. Lloyd AW, Percival D, Langille MGI, Yurgel SN. Changes to soil microbiome resulting from synergistic effects of fungistatic compounds pyrimethanil and fluopyram in lowbush blueberry agriculture. Microorganisms. 2023;11(2):410. doi:10.3390/microorganisms11020410

9. Cus F, Raspor P. Effect of pyrimethanil on the growth of wine yeasts. Lett Appl Microbiol. 2008;47(1):54–9. doi:10.1111/j.1472-765X.2008.02383.x

10. Eastabrook CL, Maqueda MM, Vagg C, Idomeh J, Nasif-Whitestone TA, Lawrence P, et al. Determining toxicity and environmental transport potential of pyridine using the brown crab Cancer pagurus. bioRxiv. 2022;516169. doi:10.1101/2022.11.17.516169

11. Bernabò I, Guardia A, Macirella R, Tripepi S, Brunelli E. Chronic exposure to the fungicide pyrimethanil: Multi-organ effects in the Italian tree frog (Hyla intermedia). Sci Rep. 2017;7:7367. doi:10.1038/s41598-017-07367-6

12. Meng Y, Zhong K, Xiao J, Huang Y, Wei Y, Tang L, et al. Developmental and cardiotoxic effects of pyrimethanil in zebrafish. Chemosphere. 2020;255:126889. doi:10.1016/j.chemosphere.2020.126889

13. Shinn C, Delello-Schneider D, Mendes LB, Sanchez AL, Müller R, Espíndola ELG, Araújo CVM. Immediate and mid-term effects of pyrimethanil toxicity on microalgae under episodic contamination. Chemosphere. 2015;120:407–13. doi:10.1016/j.chemosphere.2014.08.023

14. Aleksić M, Stanisavljević D, Smiljković M, Vasiljević P, Stevanović M, Soković M, et al. Pyrimethanil: Effective fungicide against Aspergillus rot on cherry tomato but cytotoxic to human cell lines. Ann Appl Biol. 2019;175(2):228–35. doi:10.1111/aab.12532

15. Giaever G, Chu AM, Ni L, Connelly C, Riles L, Véronneau S, et al. Functional profiling of the Saccharomyces cerevisiae genome. Nature. 2002;418:387–91. doi:10.1038/nature00935

16. Sanchez BJ, Nielsen J. Genome-scale models of yeast: Toward standardized evaluation and multi-omic integration. Integr Biol. 2015;7(8):846–58. doi:10.1039/C5IB00083A

17. Pagano L, Caldara M, Villani M, Zappettini A, Marmiroli N, Marmiroli M. In vivo–in vitro comparative toxicology of cadmium sulphide quantum dots in Saccharomyces cerevisiae. Nanomaterials. 2019;9(4):512. doi:10.3390/nano9040512

18. Vanderwaeren L, Dok R, Voordeckers K, Nuyts S, Verstrepen KJ. Saccharomyces cerevisiae as a model for eukaryotic cell biology, from cell-cycle control to DNA-damage response. Int J Mol Sci. 2022;23(19):11665. doi:10.3390/ijms231911665

19. Gillham R. Changes in mammalian abundance through the Eocene–Oligocene climate transition in the White River Group of Nebraska, USA [dissertation]. University of Nebraska–Lincoln; 2019.

20. Mendes F, Miranda E, Amaral L, Carvalho C, Castro BB, Sousa MJ, Chaves SR. Novel yeast-based biosensor for environmental monitoring of tebuconazole. Appl Microbiol Biotechnol. 2024;108(1):10. doi:10.1007/s00253-023-12944-z

21. Gil FN, Becker JD, Viegas CA. Potential mechanisms underlying pyrimethanil response in Saccharomyces cerevisiae: Gene expression profiling. J Agric Food Chem. 2014;62(23):5237–47. doi:10.1021/jf5007775

22. Thomas D, Surdin-Kerjan Y. Metabolism of sulfur amino acids in Saccharomyces cerevisiae. Microbiol Mol Biol Rev. 1997;61(4):503–32. doi:10.1128/mmbr.61.4.503–532.1997

23. Aitken SM, Lodha PH, Morneau DJK. Enzymes of the transsulfuration pathways: Active-site characterizations. Biochim Biophys Acta Proteins Proteom. 2011;1814(11):1511–7. doi:10.1016/j.bbapap.2011.03.006

24. Hansen J, Johannesen PF. Cysteine is essential for transcriptional regulation of sulfur assimilation genes in Saccharomyces cerevisiae. Mol Gen Genet. 2000;263:535–42. doi:10.1007/s004380051199

25. Sherman F. Getting started with yeast. Methods Enzymol. 2002;350:3–41. doi:10.1016/S0076-6879(02)50954-X

26. Green MR, Sambrook J. Molecular Cloning: A Laboratory Manual. 4th ed. Cold Spring Harbor (NY): Cold Spring Harbor Laboratory Press; 2012.

27. Niedenthal RK, Riles L, Johnston M, Hegemann JH. GFP as a reporter for gene expression and subcellular localization in budding yeast. Yeast. 1996;12(8):773–86. doi:10.1002/(SICI)1097-0061(19960630)12:8<773::AID-YEA972>3.0.CO;2-L

28. Costa ACT, Russo M, Fernandes AAR, Broach JR, Fernandes PMB. Transcriptional response of multi-stress-tolerant Saccharomyces cerevisiae to sequential stresses. Fermentation. 2023;9:195. doi:10.3390/fermentation9020195

29. Mat Nanyan NS, Takagi H. Proline homeostasis in Saccharomyces cerevisiae: How does the stress-responsive transcription factor Msn2 play a role? Front Genet. 2020;11:438. doi:10.3389/fgene.2020.00438

30. Martin-Yken H. Yeast-based biosensors: Current applications and new developments. Biosensors. 2020;10:51. doi:10.3390/bios10050051.

31. Tang H, Wu Y, Deng J, Chen N, Zheng Z, Wei Y, et al. Promoter architecture and promoter engineering in Saccharomyces cerevisiae. Metabolites. 2020;10:320. doi:10.3390/metabo10080320.

32. Edwards H, Yang Z, Xu P. Characterization of Met25 as a color-associated genetic marker in Yarrowia lipolytica. Metab Eng Commun. 2020;11:e00147. doi:10.1016/j.mec.2020.e00147.

33. Vopálenská I, Váchová L, Palková Z. New biosensor for detection of copper ions in water based on immobilized genetically modified yeast cells. Biosens Bioelectron. 2015;72:160–167. doi:10.1016/j.bios.2015.05.006.

34. Wahid E, Ocheja OB, Marsili E, Guaragnella C, Guaragnella N. Biological and technical challenges for implementation of yeast-based biosensors. Microb Biotechnol. 2023;16(1):54–66. doi:10.1111/1751-7915.14183.

35. Žunar B, Mosrin C, Bénédetti H, Vallée B. Re-engineering of CUP1 promoter and Cup2/Ace1 transactivator to convert Saccharomyces cerevisiae into a whole-cell eukaryotic biosensor capable of detecting 10 nM copper. Biosens Bioelectron. 2022;214:114502. doi:10.1016/j.bios.2022.114502.

36. Nemer G, Koubaa M, El Chamy L, Maroun RG, Louka N. Seeing colors: A literature review on colorimetric whole-cell biosensors. Fermentation. 2024;10:79. doi:10.3390/fermentation10020079.

37. Nisamedtinov I, Lindsey GG, Karreman R, Orumets K, Koplimaa M, Kevvai K, et al. The response of Saccharomyces cerevisiae to sudden vs. gradual environmental stress monitored by Hsp12p expression. FEMS Yeast Res. 2008;8(6):829–838. doi:10.1111/j.1567-1364.2008.00391.x.

38. Antonazzi F, Di Felice F, Camilloni G. GCN5 enables HSP12 induction promoting chromatin remodeling, not histone acetylation. Biochem Cell Biol. 2021;99(6):700–706. doi:10.1139/bcb-2020-0620.

39. Temelli N, van den Akker S, Weusthuis RA, Bisschops MMM. Exploring yeast energy dynamics: The general stress response lowers maintenance energy requirement. Microb Biotechnol. 2025;18(4):e70126. doi:10.1111/1751-7915.70126.

40. Zhang M-L, Zhang H, He Y-X, Wu Z-H, Xu K. Improving thermo-tolerance of Saccharomyces cerevisiae by precise regulation of small HSP expression. RSC Adv. 2023;13:36254–36260. doi:10.1039/D3RA05216H.

41. Dacquay LC, McMillen DR. Improving the design of an oxidative-stress-sensing biosensor in yeast. FEMS Yeast Res. 2021;21(4):foab025. doi:10.1093/femsyr/foab025.

42. Zhang Y, Shi S. Transcription factor-based biosensor for dynamic control in yeast for natural product synthesis. Front Bioeng Biotechnol. 2021;9:635265. doi:10.3389/fbioe.2021.635265.

43. Mendes F, Machado BO, Castro BB, et al. Harnessing the power of biosensors for environmental monitoring of pesticides in water. Appl Microbiol Biotechnol. 2025;109:92. doi:10.1007/s00253-025-13461-x.

44. Gutiérrez JC, Amaro F, Díaz S, Martín-González A. Environmental biosensors: A microbiological view. In: Thouand G, editor. Handbook of Cell Biosensors. Cham: Springer; 2022. doi:10.1007/978-3-030-23217-7_191.

45. Cheliukanov M, Gurkin G, Perchikov R, Medvedeva A, Lavrova T, Belousova T, et al. Whole-cell microorganisms as bioanalytical tools for pollution monitoring: A review. Biosensors. 2025;15:290. doi:10.3390/bios15050290.

46. Fan C, He N, Yuan J. Cascaded amplifying circuit enables sensitive detection of fungal pathogens. Biosens Bioelectron. 2024;250:116058. doi:10.1016/j.bios.2024.116058.

47. Sheikhi R, Dehghani MH, Nabizadeh R, Mahvi AH, Naddafi K, Ahmadikia K. Developing a Saccharomyces cerevisiae-based cytotoxicity bioassay for assessing contaminated waters. Ecotoxicol Environ Saf. 2025;299:118407. doi:10.1016/j.ecoenv.2025.118407.

48. Ocheja OB, Wahid E, Franco JH, Trotta M, Guaragnella C, Marsili E, et al. Polydopamine-immobilized yeast cells for portable electrochemical copper biosensors. SSRN. 2023. doi:10.2139/ssrn.4647249.

Received: 29 Oct 2025 / **Accepted:** 10 Dec 2025 / **Published (online):** 15 Dec 2025 (Europe/Madrid)

Citation. Robles-Ruiz P.C., Arias-Arias D.E., Álvarez F.J., Aguirre-Bravo A., Gonzales-Zubiate F.A. *Functional Characterization of the STR3 Promoter under Exposure to the Pesticide Pyrimethanil: A Potential Tool for Environmental Monitoring.* BioNatura Journal. 2025; 2(4): 20. https://doi.org/10.70099/BJ/2025.02.04.20

Additional Information

Correspondence should be addressed to: fgonzales@yachaytech.edu.ec

Peer Review Information
BioNatura Journal thanks the anonymous reviewers for their valuable contribution to the peer-review process.
Regional peer-review coordination was conducted under the BioNatura Institutional Publishing Consortium (BIPC), involving:

- Universidad Nacional Autónoma de Honduras (UNAH)
- Universidad de Panamá (UP)
- RELATIC (Panama)

Reviewer selection and assignment were supported via: https://reviewerlocator.webofscience.com/

Publisher Information
Published by Clinical Biotec S.L. (Madrid, Spain) as the publisher of record under the BioNatura Institutional Publishing Consortium (BIPC).
Institutional co-publishers:

- UNAH (Honduras)
- UP (Panama)
- RELATIC (Panama)

Places of publication: Madrid (Spain); Tegucigalpa (Honduras); Panama City (Panama)
Online ISSN: 3020-7886

Governance
For editorial governance and co-publisher responsibilities, see the BIPC Governance Framework (PDF) at:
https://clinicalbiotec.com/bipc